Sci. Bull.
DOI 10.1007/s11434-016-1098-7

www.scibull.com
www.springer.com/scp

Article

Materials Science

Selective laser melting 3D printing of Ni-based superalloy: understanding thermodynamic mechanisms

Mujian Xia · Dongdong Gu · Guanqun Yu · Donghua Dai · Hongyu Chen · Qimin Shi

Received: 6 March 2016 / Revised: 21 April 2016 / Accepted: 27 April 2016

Abstract A mesoscopic model has been established to investigate the thermodynamic mechanisms and densification behavior of nickel-based superalloy during additive manufacturing/three-dimensional (3D) printing (AM/3DP) by numerical simulation, using a finite volume method (FVM). The influence of the applied linear energy density (LED) on dimensions of the molten pool, thermodynamic mechanisms within the pool, bubbles migration and resultant densification behavior of AM/3DP-processed superalloy has been discussed. It reveals that the center of the molten pool slightly shifts with a lagging of 4 μm towards the center of the moving laser beam. The Marangoni convection, which has various flow patterns, plays a crucial role in intensifying the convective heat and mass transfer, which is responsible for the bubbles migration and densification behavior of AM/3DP-processed parts. At an optimized LED of 221.5 J/m, the outward convection favors the numerous bubbles to escape from the molten pool easily and the resultant considerably high relative density of 98.9 % is achieved. However, as the applied LED further increases over 249.5 J/m, the convection pattern is apparently intensified with the formation of vortexes and the bubbles tend to be entrapped by the rotating flow within the molten pool, resulting in a large amount of residual porosity and a sharp reduction in densification of the superalloy. The change rules of the relative density and the corresponding distribution of porosity obtained by experiments are in accordance with the simulation results.

Keywords Selective laser melting · 3D printing · Mesoscopic simulation · Thermodynamics · Densification · Porosity

M. Xia · D. Gu (✉) · G. Yu · D. Dai · H. Chen · Q. Shi
College of Materials Science and Technology,
Nanjing University of Aeronautics and Astronautics,
Nanjing 210016, China
e-mail: dongdonggu@nuaa.edu.cn

M. Xia · D. Gu · G. Yu · D. Dai · H. Chen · Q. Shi
Institute of Additive Manufacturing (3D Printing),
Nanjing University of Aeronautics and Astronautics,
Nanjing 210016, China

1 Introduction

Nickel-based superalloys are known as an attractive candidate for many industrial applications, e.g., gas turbine disks, rocket motors, spacecraft, etc., due to their excellent hot resistance to oxidation, high strength and wear resistance [1–4]. However, since superalloys have the high abilities of self-hardening and retaining superior mechanical properties at high temperatures, they are difficult to be manufactured by conventional processing methods, caused by severe tool wear damage, low material removal rate, poor thermal property and surface integrity [5–8].

The newly developed selective laser melting (SLM) additive manufacturing/3D printing (AM/3DP) technology, due to the possibility to fabricate the geometrically complex components by user-defined computer aided design (CAD) data files without tools or molds, has been proved to be an effective and economical method for processing Ni-based superalloys [9–11]. The as-built components having high dimensional precision, perfect surface quality and outstanding performance can be achieved precisely by AM/3DP [12–15]. A number of previous attempts concerning the wear resistance, high-temperature oxidation and mechanical properties of AM/3DP Ni-based superalloys have been investigated systematically [16–18]. Some typical defects such as pore [19] and residual stress [20] have been observed in as-fabricated components, limiting its further applications in the practical industrial fields. Porosity is regarded as a commonly existed processing defect that is usually observed in a majority of the metallic parts processed by AM/3DP [21, 22], which results in the poor densification level and/or other mechanical properties [19, 23]. Many previous studies have ascribed the porosity formation to the following phenomena including powder denudation [24], collapse of key holes [25], gaseous bubbles entrapment [26], incomplete re-melting of some local sites [27] and splash [28]. Actually, for the bubbles migration and porosity formation, it is difficult to be monitored or characterized within the dynamic molten pool during AM/3DP. So far, only few previous researches have been reported on this issue. For instance, Dai and Gu [29] have established a new model to investigate the densification behavior of Cu-based composites by considering the migration and escaping of bubbles. Nevertheless, there still lacks of a relatively clear and comprehensive understanding of the physical mechanisms for AM/3DP of Ni-based superalloys. It is therefore necessary to give a thermodynamic investigation on porosity evolution and densification behavior of AM/3DP-processed superalloys.

In this paper, the influence of linear energy density (LED) of laser on the thermodynamic behavior, bubbles migration behavior and densification mechanism of AM/3DP processed Ni-based superalloy was numerically studied by applying commercially computational fluid dynamics (CFD) software. To further validate the accuracy of the newly developed mesoscopic model and to acquire the optimal SLM AM/3DP processing parameters to fabricate components with higher densification, the relative density of the parts predicted by the numerical simulation was compared with the experimental results.

2 Modeling approach and experimental procedures

2.1 Physical model

During SLM processing, the interaction between laser beam and powder in the shield gas ambient is extremely complex [30, 31]. Regarding the migration of gaseous bubbles and attendant densification mechanism of powder, a schematic of SLM physical model is depicted in Fig. 1a.

Recently, the powder-scale model, i.e., the mesoscopic model, has been established to study the porosity evolution and surface morphology of titanium alloy during SLM [23]. In our present study, the powder system, processed in 3D size of (400 × 180 × 50) μm^3 (*X*-, *Y*-, *Z*-axis), contains a mixture of Ni-based superalloy powder particles and argon gaseous bubbles, as shown in Fig. 1b. A number of powder particles (average diameter of 30 μm) were closely

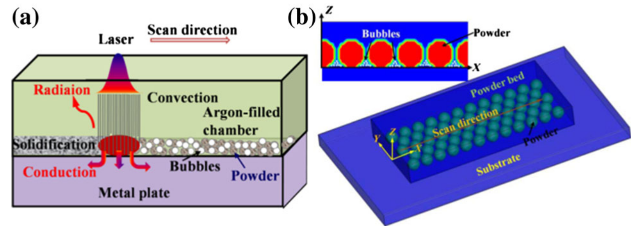

Fig. 1 (Color online) Schematic of SLM physical model (**a**) and the 3D model established for simulating SLM process (**b**)

packed in powder bed with a relative packed density of powder up to 47 %, which is close to the theoretical packed density of 55 % of the spherical powder particles [32].

2.2 Governing equations

Generally, the movement of melt fluid is followed by the mass, momentum and energy conservation, which can be written as follows [33]:

$$\frac{\partial \rho}{\partial t} + \frac{\partial(\rho u)}{\partial X} + \frac{\partial(\rho v)}{\partial Y} + \frac{\partial(\rho w)}{\partial Z} = 0, \quad (1)$$

$$\rho\left(\frac{\partial \vec{V}}{\partial t} + \vec{V} \cdot \nabla \vec{V}\right) = \mu \nabla^2 \vec{V} - \nabla p \vec{V} + M_s \cdot \vec{V} + F, \quad (2)$$

$$\rho\left(\frac{\partial T}{\partial t} + \vec{V} \cdot \nabla T\right) = \nabla \cdot (\kappa \nabla T) + S_H, \quad (3)$$

where ρ, κ, μ and p represent density, thermal conductivity, dynamic viscosity and pressure, respectively. ∇T is the temperature gradient distributed along the 3D coordinates, $\vec{V}$ is the motion velocity of the melt, M_s is the mass source, and $\vec{F}$ refers to the body force. S_H is the source term of the energy equation in the *X*, *Y* and *Z* axis and can be defined by

$$S_H = -\rho\left(\frac{\partial}{\partial t} \Delta H + \nabla \cdot (\vec{V} \Delta H)\right), \quad (4)$$

where ΔH is the latent heat of phase transformation.

Based on the volume of fluid (VOF) model applied in this simulation, the volume fraction equation for *i* phase is [34]

$$\frac{\partial \alpha_i}{\partial t} + \vec{v} \cdot \nabla \alpha_i = \frac{S_{\alpha_i}}{\rho_i}, \quad (5)$$

where $\sum_{i=1}^{n} \alpha_i = 1$, α_i represents the volume fraction of *i* phase, *n* is the total number of phases.

2.3 Boundary conditions

The transient spatial temperature distribution *T*(*x*, *y*, *z*, *t*) is time-dependent. Prior to SLM process, the initial condition of the uniform temperature distribution throughout the powder bed at $t = 0$ can be settled as